Available online at www.sciencedirect.com
SCIENCE DIRECT®
International Journal of Mass Spectrometry 229 (2003) 99–106
International Journal of Mass Spectrometry
www.elsevier.com/locate/ijms

Turn-over frequencies of catalytic reactions on nanocatalysts measured by pulsed molecular beams and quantitative mass spectrometry

Ken Judai, Stéphane Abbet, Anke S. Wörz, Martin A. Röttgen, Ueli Heiz*

Institute of Surface Chemistry and Catalysis, University of Ulm, Albert-Einstein-Allee 47, 89069 Ulm, Germany

Received 24 January 2003; accepted 11 March 2003

Abstract

We present an experimental scheme for measuring turn-over frequencies (TOFs) and obtaining mechanistic details of catalytic processes on small clusters on surfaces with high sensitivity. The scheme uses a newly designed pulsed, piezo-electric driven valve with extremely high pulse-to-pulse stability in combination with quantitative mass spectrometry. The experimental scheme is applied for studying the oxidation of CO on mass-distributed palladium clusters deposited from a molecular beam onto well-characterized oxide surfaces. The obtained results are compared to the ones of palladium single crystals and supported palladium particles on oxide surfaces. The measured TOF is 47 ± 8 CO_2 molecules per deposited atom per second at 350 K and the observed mechanistic details can be explained by different active centers on the clusters and by the competitive adsorption of the two reactant molecules. The interpretation is in agreement with earlier studies on the oxidation of CO on palladium model catalysts.

Keywords: TOF; Nanocatalysis; Quantitative mass spectrometry; CO-oxidation; Palladium clusters

1. Introduction

In the last decade the study of nanocatalysis has become a growing field of research [1–4]. In nanocatalysis two important conditions have to be fulfilled [5]. First, the valence electrons of the active part of a nanocatalyst are highly confined leading to physical and chemical properties non-scalable from bulk properties. This condition is true for clusters/particles in the nanometer length scale or smaller. Second, nanocatalysts are designed in a controlled manner. The exploration of material properties in the non-scalable regime has profound consequences. Atomic clusters, e.g., exhibit unique, size-dependent electronic [6], magnetic [7,8], and chemical properties [9,10] that differ from those of bulk materials. In contrast to supported particles of larger size or extended solid surfaces, small clusters adsorbed at specific sites of a support material change their intrinsic properties to a large extend, in particular when charging of the cluster occurs. Nanocatalysts exhibit remarkable quantum size effects and structural fluxionality. This opens new avenues for atom-by-atom design of nanocatalysts whose chemical activity, specificity, and selectivity can be tuned by controlling the cluster size, through the incorporation of impurity atoms, and via manipulation of the strength of the cluster–support interaction, the degree of charging of the cluster, and by changing their magnetic properties [11–13].

In the last couple of years we designed nanocatalysts by depositing small, size-selected clusters on well-defined oxide surfaces and studied their chemical properties [13–17]. Remarkable size effects were discovered, chemical reactions, however, have been studied so far by one-cycle experiments only [18]. Thus, an experimental proof that these systems are active for catalytic processes, e.g., several cycles of a catalytic reaction are promoted without destroying the catalysts, is still missing. Here we present an experimental scheme to study catalytic processes of clusters on surfaces with high sensitivity. We use a newly designed pulsed valve with excellent pulse-to-pulse stability in combination with absolutely calibrated mass spectrometry to determine turn-over frequencies (TOFs) for the oxidation of CO on size-distributed Pd clusters. Due to its importance in cleaning hydrocarbon combustion exhausts or in the CO removal in fuel cells, the CO-oxidation reaction is one of the most studied catalytic process over a variety of transition metals

* Corresponding author.
E-mail address: ulrich.heiz@chemie.uni-ulm.de (U. Heiz).

1387-3806/$ – see front matter © 2003 Elsevier B.V. All rights reserved.
doi:10.1016/S1387-3806(03)00261-6

and the mechanism of the reaction has been well established. By using molecular beam techniques, Engel and Ertl were able to demonstrate that the reaction on palladium surfaces follows a Langmuir–Hinshelwood mechanism and that the reaction rate as function of temperature is independent on the crystallographic orientation of the surface [19,20]. From this they concluded that the reaction is structure-insensitive. On palladium model catalysts, the reaction has also been extensively studied, the evolution of the reaction rates with size, however, has still not been determined on a molecular level. Boudart has shown that in general the rate of a structure-insensitive reaction is independent of particles size and thus the single crystal studies point towards a size independent reaction [21]. Stara et al., however, have found indications for significant size effects by studying the transient CO_2 formation on Pd/Al_2O_3 model catalysts [22]. In contrast, similar effects have not been observed in a recent work by Libuda et al. on the same model system [23]. On Pd/MgO(1 0 0), investigations carried out by Henry and coworkers show the reaction rate to display strong dependence on particle size and particle density [24–26]. This dependence can, however, mainly be explained by the reverse-spillover of CO from the support to the particles, which increases the effective CO pressure on the particles when particle size decreases. With the presented experimental scheme it will in the future be possible to study these questions on size-selected clusters on surfaces [27] and hopefully this will lead to an molecular understanding of the size effects for the oxidation of CO by palladium.

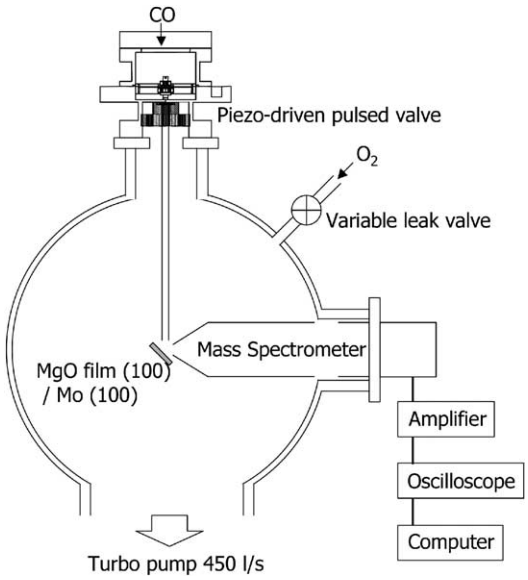

Fig. 1. Experimental scheme of the relevant elements for performing pulsed molecular beam experiments. Shown is the UHV chamber with the pulsed piezo-electric valve, the variable leak valve and the absolutely calibrated mass spectrometer. The cluster sample is mounted on the vertical axis of the chamber by a *x*, *y*, *z*-manipulator. The signal is amplified by a multichannel plate and the preamplifier of the mass spectrometer and subsequently recorded by a digital oscilloscope interfaced to a PC.

2. Experiment

2.1. Overview

Palladium clusters are produced by a recently developed high-frequency laser evaporation source [18]. In this setup the output (355 nm) of a Nd:YAG laser is focused onto a rotating Pd target disk. A helium pulse thermalizes the produced metal plasma, and the clusters are grown by nucleation when the helium–metal vapor undergoes supersonic expansion. Subsequently, the positively charged cluster ions are guided by home-build ion optics through differentially pumped vacuum chambers. In contrast to the ion optics described in [18] we replaced the first set of Einzel lenses by a home-built octo-pole ion guide [28,29], this augmented the transmittance by a factor of 2 and increased the stability of the cluster beam. With this apparatus monodispersed clusters with masses of up to 9000 amu can be deposited after size-selection with a quadrupole mass spectrometer (ABB-Extrel; mass limit: 1000, 4000, and 9000 amu). In this paper we focus on mass-distributed clusters (Pd_x; $x = 55 \pm 25$), which are deposited with low kinetic energy (0.1–2 eV) onto magnesium oxide (MgO) thin films, mass-distributed clusters were used in order to compare obtained TOF for the CO-oxidation with experimental values described in the literature [26,30]. Investigations on size-selected clusters are in progress [27]. The cluster ions are neutralized upon impact either on defect sites (F, F^+ center) or by charge tunneling through the thin MgO films [31]. We deposited 1% of a monolayer (ML) of mass-distributed Pd clusters ($1\,ML = 2.2 \times 10^{15}$ clusters/cm^2) at 90 K to land them isolated on the surface and to prevent agglomeration on the MgO films. The support is prepared in situ for each experiment by evaporating magnesium in an oxygen (O_2) background and by annealing the sample subsequently to 800 K [32]. These thin films (~10 MLs) show bulk-like structural and electronic properties as observed by low electron energy diffraction (LEED), X-ray photoelectron spectroscopy (XPS), UV photoelectron spectroscopy (UPS), and electron energy loss spectroscopy (EELS) [2,4].

2.2. Analysis chamber

A systematic view of the elements of the analysis chamber relevant to this work is depicted in Fig. 1. The deposited clusters can be exposed to different reactant gases by two kinds of valves. First, it can be exposed isotropically to, e.g., O_2 by a commercial, ultra-high vacuum (UHV) compatible, variable leak valve. Second, reactant molecules (e.g., CO) can be introduced via a pulsed molecular beam produced by a home-made, piezo-electric driven, pulsed valve. This pulsed valve has a high pulse-to-pulse stability (time profile), and allows studying catalytic processes on supported clusters at relatively high pressures (up to 10^{-2} mbar). Furthermore,

a stainless steal tube is attached to the pulsed nozzle in order to collimate the molecular beam and to expose the reactant molecules to the substrate only. The pulse duration at the position of the sample can in principle be varied from 1 ms up to continuous operation. For the experiments described in this work a constant pulse duration of about 40 ms were used. The repetition rate of the pulsed valve can be up to 100 Hz. The experiments were carried out at 0.1 Hz; the 10 s interlude allows the reactant gas to be pumped completely.

After ejecting the CO molecule to the substrate at a constant isotropic pressure of O_2 (5×10^{-7} mbar), the resulting product molecules (CO_2) were detected by an absolutely calibrated quadruple mass spectrometer. The differentially pumped, computer-controlled mass spectrometer (Balzers QMG 421) is mounted in line-of-sight with the sample. At the entrance, near the ionizer of the quadruple mass spectrometer, a skimmer with an opening of 3 mm is mounted. The skimmer is biased to −150 V in order to prevent electron-stimulated desorption induced by emitting electrons from the ionizer of the mass spectrometer. After amplifying the ion current with a multichannel plate detector, the output of the preamplifier (Balzers, EP 112) is recorded and averaged by a digital oscilloscope (Tektronix TDS320) interfaced to a personal computer.

In addition, the analysis chamber is equipped with a Fourier transform infrared spectrometer, a hemispherical electron energy analyzer used for Auger electron spectroscopy, a sputter source, two e-beam evaporators and a hot filament evaporator for thin film preparation as well as ion optics for cluster deposition.

2.3. Performance of the pulsed valve

Essential for these measurements is the home-made, pulsed valve based on the design of Proch and Trickl [33], which consists of a piezo-electric disc translator (Physics Instruments; P-286.23) with a plunger attached to its center. An applied voltage pulse causes the plunger to be moved reproducibly. A Viton O-ring glued to the plunger guarantees the tightness of the valve. Typically, a voltage of −560 V is applied to the piezo-disc for a duration of 150 μs. The duration can however be chosen in a large time range and when applying a dc-voltage the valve can be used as a continuous, highly precise and reproducible leak valve. For the experiments described here the backing pressures was 1 bar. For each pulse the stagnated gas is then injected into the vacuum through a 0.7 mm diameter hole. As in our setup the pulsed valve cannot be mounted close to the sample and as the divergence of the molecular beam is non-negligible, a tube (inner diameter: 4 mm, length: 300 mm) is mounted to the valve in order to collimate the molecular beam to the substrate; due to the limited conductance of the tube the pulse width is increased by a factor of 5. For these conditions the performance of the valve is summarized in Fig. 2 showing shape and time profile of the molecular beam, respectively. The full width at half maximum (FWHM) of the beam at the position of the substrate (5 mm from the exit of the tube) is 10 mm (Fig. 2a), this corresponds to the diameter of the used substrate (MgO(1 0 0) thin films grown on a Mo(1 0 0) single crystal). The corresponding time profile is shown in Fig. 2b with an observed FWHM of around 40 ms, without tube it is about 20 ms. The flux of the valve was calibrated by measuring the decrease of the stagnation pressure with time, operating the valve at 10 Hz for 24 h. From this calibration we obtain a value of 5.1×10^{15} molecules/pulse. Taking the beam shape and time profile into account, an effective maximal pressure at the substrate of 2×10^{-4} mbar is obtained. Most important for these experiments is the excellent pulse-to-pulse stability of the beam and time profile. Fig. 2c depicts several shots of the valve, where gas pulses (CO) were measured without averaging. The shape of the observed time profile is identical for all pulses and the integrals of the single pulses (proportional to the total number of exciting molecules) are constant within 1%. This stability is essential for studying the catalytic properties of cluster model catalysts as (a) the time-dependent coverage of the reactants is identical for each pulse and the time evolution of the catalytic properties can be studied over a long time period, (b) the sensitivity of the experimental scheme can be increased by averaging many pulses supposing the catalytic process is time-invariant, and (c) the signal-to-noise of the obtained kinetics (concentration profile of the reactants and products measured at several temperatures) is enhanced, allowing the data to be simulated by several techniques (fast Fourier transformation, numerical integration of the differential rate equations, etc.) [27] to obtain details of reaction mechanisms.

2.4. Measuring turn-over frequencies

The TOFs for the oxidation of CO on size-distributed Pd_x clusters ($x = 55 \pm 25$) are measured in the following way. On a freshly prepared MgO(1 0 0) thin film, 1% ML (1 ML = 2.2×10^{15} cm^{-2}) of Pd clusters were deposited. The coverage of the clusters is known with high precision as the cluster current is integrated during deposition. The vacuum chamber is then filled with a given partial pressure of O_2 (1×10^{-8} mbar $< p_{Oxygen} < 2 \times 10^{-6}$ mbar), resulting in an isotropic O_2 exposure on the cluster sample. The pulsed valve is then turned on and operated at 0.1 Hz. For each pulse the sample is first dosed with a strongly anisotropic CO pulse from the highly directed molecular beam; the maximal, effective pressure on the sample is 2×10^{-4} mbar; subsequently the sample is exposed to the isotropic contribution of backscattered reactant molecules. The anisotropic and isotropic contributions can easily be disentangled by first putting the sample in front of the mass spectrometer (Fig. 3a, solid line: the measured CO signal consists of both contributions) and then taking the sample out of this position (Fig. 3a, dotted line: the measured signal consists of the isotropic contribution only). The difference spectrum shown in Fig. 3b is the anisotropic contribution only. As

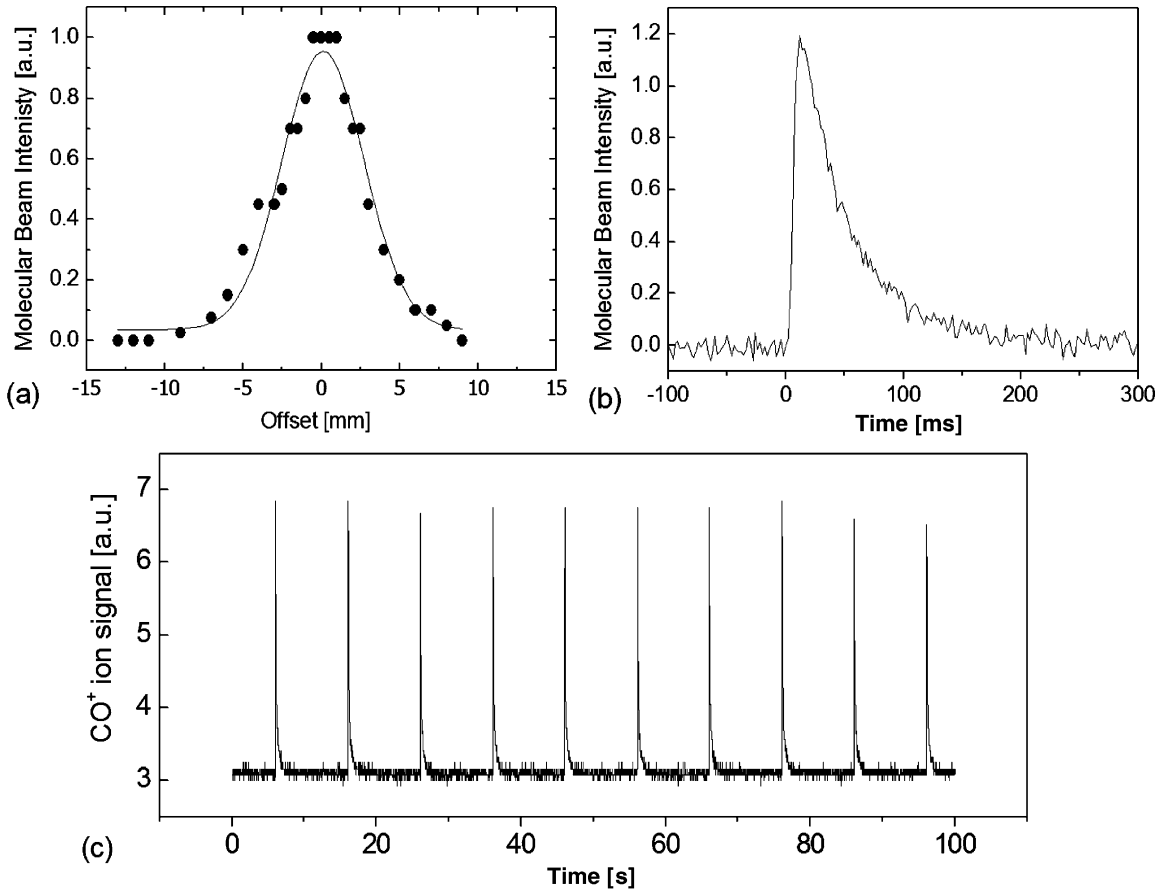

Fig. 2. Shown are some characteristics of the molecular pulses of the piezo-electric valve: beam profile (a), time profile (b), and pulse-to-pulse stability (c).

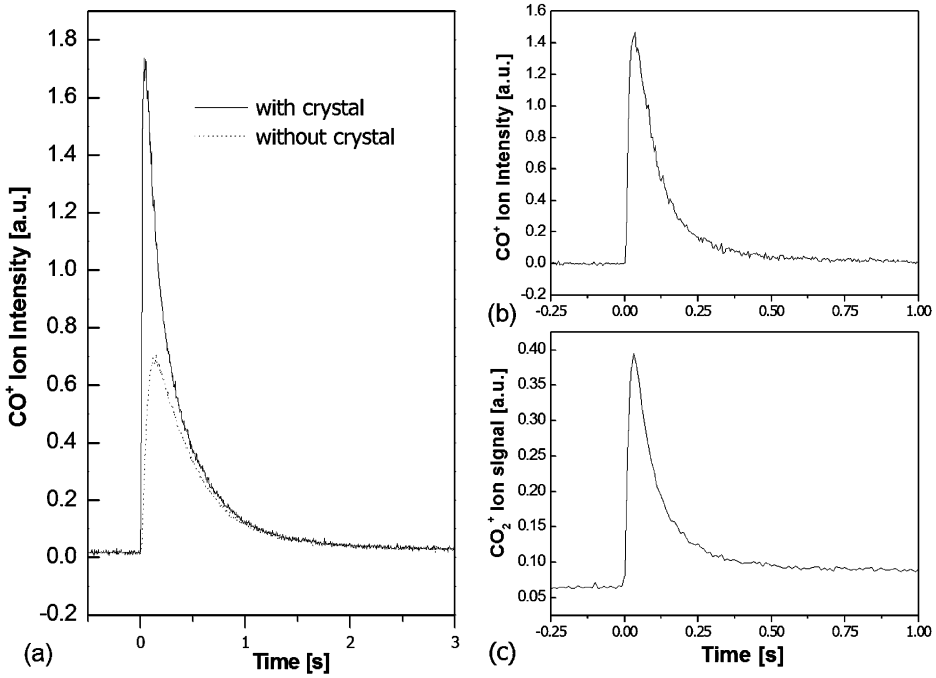

Fig. 3. (a) Shown is the measured CO^+ ion intensity with the cluster sample in position (solid line) and out of position (dotted line). (b) The difference spectrum results in the anisotropic contribution of the CO exposure on the sample, see text. Note that the shape of the anisotropic contribution is similar to the shape of the formed CO_2 at a constant oxygen background (c).

expected the isotropic contribution is smaller and timely delayed (∼10 ms). For each pulse the product molecule, CO_2, can then be detected by the mass spectrometer. A typical time profile is shown in Fig. 3c. Here it is worth mentioning that the FWHM of the time profile of CO_2 is very similar to the one of the anisotropic exposure of CO shown in Fig. 3b but considerably smaller than the one of the isotropic contribution. Thus, the effective pressure of the isotropic contribution of CO on the sample is too low the oxidation reaction to occur and is therefore neglected for further considerations.

More important for this work is the evaluation of the integral of the CO_2 pulse. We absolutely calibrated our mass spectrometer by measuring the reflected CO from the MgO substrate of a known pulse from the piezo-electric valve; this method is accurate, as we did not observe any reactive scattering, e.g., formation of CO_2 by the reaction of CO with oxygen atoms from the MgO substrate. The error of this measurement is estimated to be about 10%. As we also know the cluster density on the surface (see above) we can obtain TOF for the oxidation of CO by simply calculating the ratio of the total number of formed CO_2 and the number of clusters on the surface times the pulse duration. The TOF is an important property of a catalytic process and in the following we are presenting these numbers for various conditions, e.g., partial pressures of the reactants and temperatures to characterize this reaction on size-distributed Pd clusters in detail and in order to learn important mechanistic details.

3. Results and discussions

So far, it has been an open question whether such small clusters on surfaces indeed remain stable after a single catalytic reaction, a necessary condition in catalysis. These transient molecular beam experiments (carried out at the conditions described above) on palladium nanocatalysts, which are formed by depositing 1% ML (1 ML = 2.2×10^{15} atoms/cm^2) of mass-distributed Pd_x clusters ($x = 55 \pm 25$) on a MgO(1 0 0)/Mo(1 0 0) thin film indeed reveal that first the nanocatalysts are active for at least 1 h (longest period of the performed experiments) at around room temperature and second that during this period the formation of CO_2 is nearly constant. In these experiments no CO_2 could be detected on clean MgO(1 0 0) thin films. In detail, Fig. 4 shows the evolution of the CO_2 pulses for various sample temperatures and for a constant, isotropic oxygen background pressure (5×10^{-7} mbar). Below ∼250 K, no CO_2 formation is observed. At 269 K, a small narrow CO_2 pulse is detected. For all temperatures only a single, averaged CO_2 pulse (30 samples) from an extended series is shown. The intensity of this peak increases up to about 408 K, where the intensity reaches the maximal value. The intensity decreases for higher temperatures and disappears at 709 K. At 307 K, a broad second, delayed peak (between 2 and 4 s) is detected. This second peak is also present at 327 and 356 K, however shifts towards shorter times. In addition, the width is clearly decreasing with temperature (see below). The TOFs as function of temperature are obtained by integrating the CO_2 pulses and dividing the obtained value by the number of deposited clusters and the width of the CO pulses (reaction time). For this procedure the mass spectrometer has been calibrated using the procedure described in the experimental section and taking the different sensibilities for CO and CO_2 into account. The number of deposited clusters was obtained by integrating the measured ion cluster current over the deposition time. This procedure results in accurate TOFs for size-selected and mass-distributed clusters. The absolute TOFs [number of CO_2 molecules/number of Pd atoms × s] for the present study are displayed in the inset of Fig. 4. The maximal TOF of the size-distributed Pd clusters is 47 ± 8. The maximal TOF of palladium model catalysts consisting of larger Pd particles (2.8 and 13 nm in diameter) on MgO(1 0 0) show much lower values (0.12), these TOFs, however, were measured at steady-state conditions [26]. Pd model catalysts consisting of similar sized Pd particles on SiO_2 revealed higher TOFs (20–2000) when measured at high pressures (1.5 Torr) [34]. The asymmetrical shape of the temperature-dependent curve is comparable to the curves measured on single crystals and model catalysts, but interestingly the maximum is shifted by 100 K to lower temperatures. In fact, the nanocatalysts consisting of small Pd clusters reveal maximal TOF at around 380 K whereas on single crystals or model catalysts maximal reactivity is observed at around 500 K. The atom-by-atom cluster size dependency and the study of possible reasons for this behavior is under investigation. Such a shift in temperature was also observed for small unsupported Pt clusters, where the CO-oxidation was studied in the gas phase and compared to real catalysts [35]. To explain the asymmetric shape we use the same arguments as for larger Pd particles on oxide surfaces [23–26]. Below 380 K, the TOFs decrease because on the one hand, the activation energy for the CO_2 formation is not reached and on the other hand, CO coverage is important (enhanced CO sticking coefficient at low temperature) and blocks oxygen adsorption. In contrast, above 380 K the smaller TOFs can be explained by the low CO coverage (decreased CO sticking coefficient at high temperatures); at elevated temperatures cluster diffusion cannot be excluded, which may also alter the TOFs in this temperature range.

Let us turn now our attention to the second, delayed CO_2 peak. Fig. 5 shows the evolution of this peak as function of temperature at constant oxygen background pressure (5×10^{-7} mbar). As already noted, the delayed peak appears at 307 K, at this temperature it is broadest and has a delay time of about 3 s. At higher temperatures the peak becomes narrower, increases in intensity and the maximum of the peak shifts to shorter delay times. Finally, at around 408 K, this peak merges into the main peak. The evolution of the delayed peak was also studied as function of the oxygen background pressure at 317 K (Fig. 6). With increasing oxygen pressure the delayed peak follows qualitatively the same

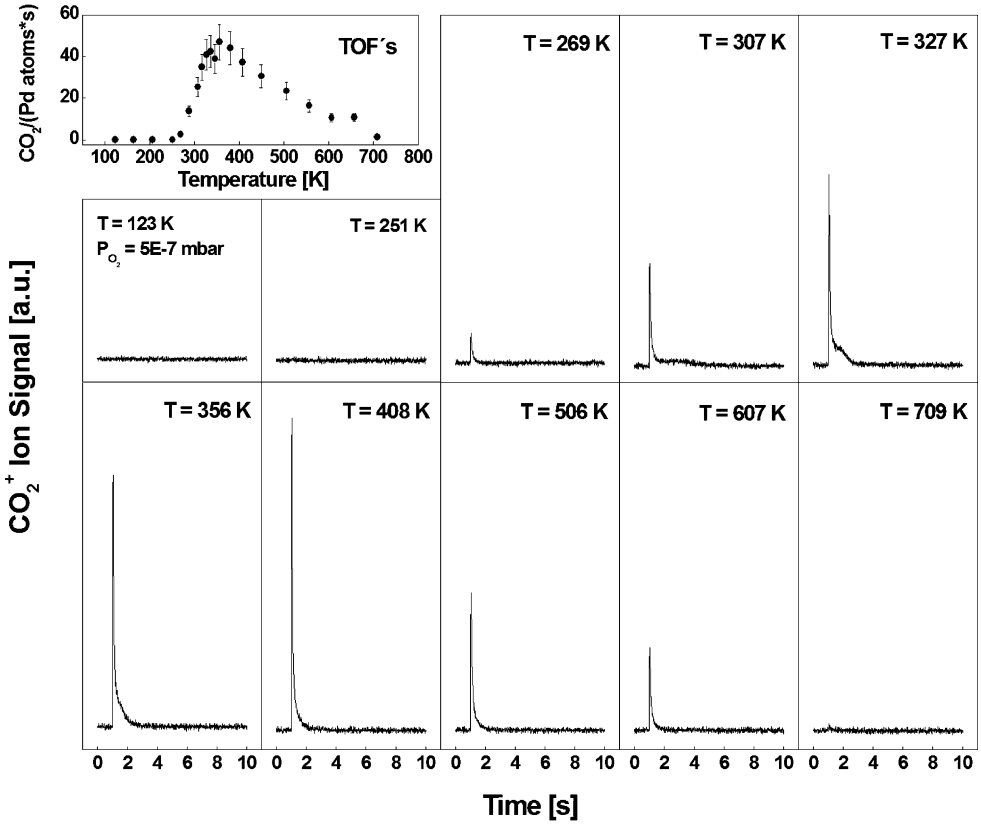

Fig. 4. Shown is the formation of CO_2 at various reaction temperatures and at a constant O_2 pressure of 5×10^{-7} mbar. The TOFs shown in the inset are obtained by integrating the CO_2 peaks and normalizing with the cluster density.

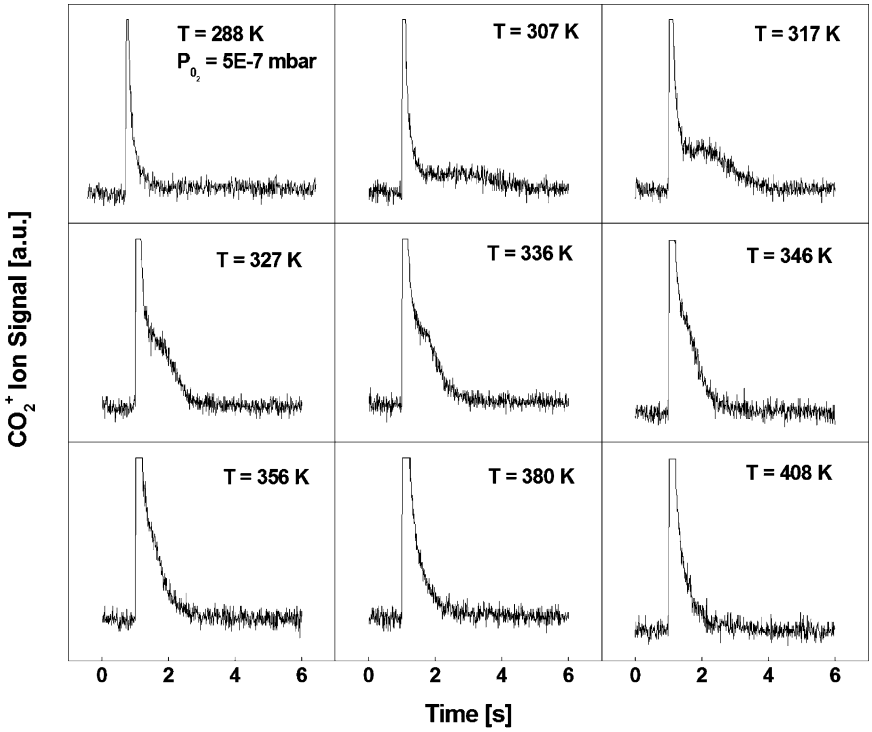

Fig. 5. Shown is the CO_2 formation at temperatures between 288 and 408 K at an oxygen pressure of 5×10^{-7} mbar. Note the appearance of a delayed peak at 307 K and the evolution of the shape and delay with temperature.

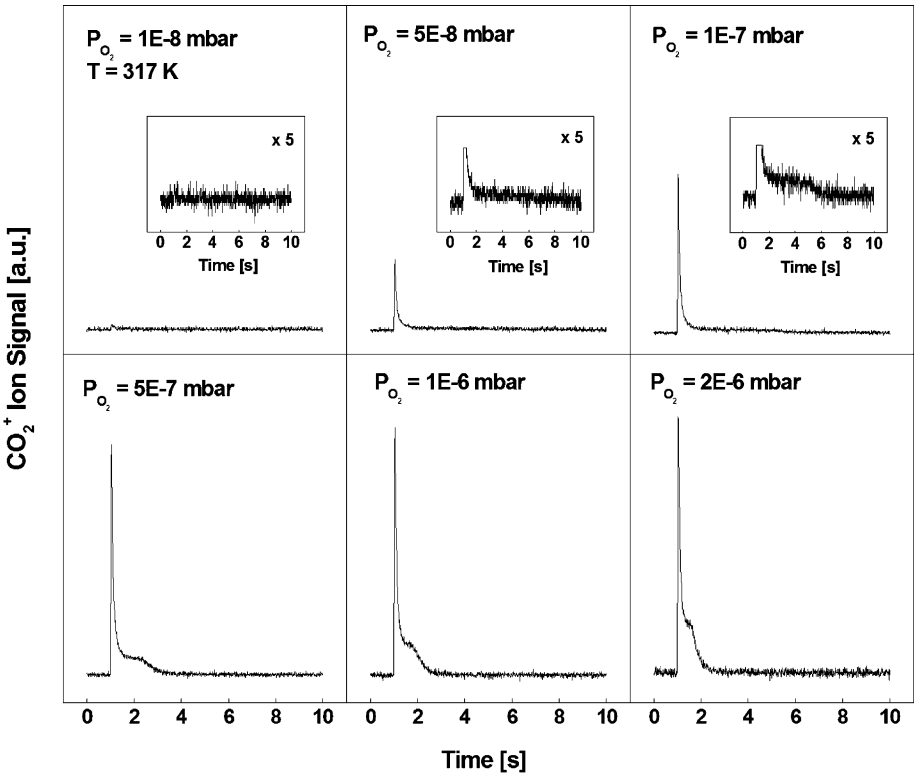

Fig. 6. Shown is the formation of CO_2 at variable oxygen pressure, p_{O_2} ($p_{O_2} = 1 \times 10^{-8}$ to 2×10^{-6} mbar) and at a constant temperature of 317 K. Note again the appearance of a delayed peak and its evolution with p_{O_2}.

evolution, e.g., the delayed peak becomes narrower, gains intensity and appears at shorter delays. Note that the first peak is observed only when the oxygen pressure is at least 5×10^{-8} mbar and that it saturates at 5×10^{-7} mbar. Above this pressure, a further increase enhances the CO_2 formation at short delay times (main peak). Whereas the origin of the first CO_2 peak is straight forward to explain (direct oxidation of the CO pulse), the explanation of the delayed peak is less obvious. The evolution of the delayed peak with temperature and oxygen pressure is very similar to the delayed formation of CO_2 first observed by Henry and coworker in transient molecular beam experiments on Pd/MgO(1 0 0) model catalysts [24–26]. In these experiments the delayed CO_2 formation appears after the CO beam is closed, while oxygen is still supplied to the sample. This peak has been explained by the presence of CO strongly bound to the particle edges. This strongly bound CO reacts well after the weakly adsorbed CO on the facets. More recently Libuda et al. have observed the same delayed peak on Pd/Al_2O_3 model catalysts [23]. By combining molecular beam experiments and time-resolved infrared reflection spectroscopy, they have shown, however, that the delayed formation of CO_2 does not originate from the presence of specific adsorption sites with high CO binding energies, but from competitive adsorption of the reactant molecules, oxygen and carbon monoxide. On the one hand, the formation of CO_2 decreases immediately after closing the CO beam as most of the adsorbed CO is going to be oxidized. On the other hand, the oxygen adsorption rate is increased when the CO coverage is lowered. Thus, a second delayed peak is observed. In the present study, the two proposed explanations (more strongly bound CO or competition between two processes) may contribute to the delayed formation of CO_2 on small palladium clusters. Future studies on mass-selected clusters in combination with kinetic simulations will reveal to what extend the two mechanisms contribute to the overall reaction mechanism of the CO-oxidation on well-defined nanocatalysts [27].

4. Conclusions

We introduced a new experimental scheme using piezo-electric driven, pulsed valves to study catalytic processes on nanocatalysts in UHV conditions. The concept of our approach is similar to the one used by Henry and coworkers, the use of the pulsed valves with the excellent pulse-to-pulse stability prevents the need of high cost differential pumping used in molecular beam techniques. We showed that this technique is sensitive enough to study catalytic processes on small clusters on oxide surfaces at coverages down to less the 0.1% ML. This opens the possibility to study catalytic processes on size-selected clusters on surfaces in order to investigate the importance of size effects in catalysis. We obtained TOF for the oxidation of CO under various experimental conditions, this is important to compare the catalytic activity of cluster catalysts with other

model catalysts and real catalysts. In addition, these studies will allow in the future for obtaining mechanistic information of a catalytic reaction by using kinetic simulations.

Acknowledgements

This work was supported by the Deutsche Forschungsgemeinschaft. K.J. thanks the Humboldt foundation for financial support, S.A. thanks the Swiss National Science foundation and the Humboldt foundation for financial support. A.S.W. acknowledges support of the Graduiertenkolleg 'Molekulare Organisation und Dynamik an Grenz- und Oberflächen'. We also thank Claude Henry for fruitful discussions.

References

[1] B.J. McIntyre, M. Salmeron, G.A. Somorjai, Science 265 (1994) 1415.
[2] U. Heiz, W.-D. Schneider, J. Phys. D (2000).
[3] U. Heiz, W.-D. Schneider (Eds.), Physical Chemistry of Supported Clusters, Springer Series in Cluster Physics, Heidelberg, 2000.
[4] U. Heiz, W.-D. Schneider, Crit. Rev. Solid State Mater. Sci. 26 (2001) 251.
[5] S. Abbet, U. Heiz, in: H.S. Nalwa (Ed.), Encyclopedia in Nanoscience and Nanotechnology, American Scientific Publishers, vol. X, 2003, p. 1.
[6] W.D. Knight, K. Clemenger, W. de Heer, W.A. Saunders, M.Y. Chou, M.L. Cohen, Phys. Rev. Lett. 52 (1984) 2141.
[7] I.M.L. Billas, A. Chatelain, W.A. de Heer, Science 265 (1994) 1682.
[8] M. Moseler, H. Häkkinen, U. Landman, Phys. Rev. Lett. 89 (2002) 176103.
[9] A. Kaldor, D. Cox, M.R. Zakin, Adv. Chem. Phys. 70 (1988) 211.
[10] L.D. Socaciu, J. Hagen, T.M. Bernhardt, L. Wöste, U. Heiz, H. Häkkinen, U. Landman, J. Am. Chem. Soc. (2003), in press.
[11] H. Häkkinen, S. Abbet, A. Sanchez, U. Heiz, U. Landman, Angewandte Chemie Int. Ed. 42 (2003) 1297.
[12] A. Sanchez, S. Abbet, U. Heiz, W.-D. Schneider, H. Häkkinen, R.N. Barnett, U. Landman, J. Phys. Chem. A 103 (1999) 9573.
[13] S. Abbet, A. Sanchez, U. Heiz, W.-D. Schneider, A.M. Ferrari, G. Pacchioni, N. Rösch, J. Am. Chem. Soc. 122 (2000) 3453.
[14] U. Heiz, F. Vanolli, A. Sanchez, W.-D. Schneider, J. Am. Chem. Soc. 120 (1998) 9668.
[15] U. Heiz, A. Sanchez, S. Abbet, W.-D. Schneider, J. Am. Chem. Soc. 121 (1999) 3214.
[16] S. Abbet, A. Sanchez, U. Heiz, W.-D. Schneider, J. Catal. 198 (2001) 122.
[17] S. Abbet, U. Heiz, H. Häkkinen, U. Landman, Phys. Rev. Lett. 86 (2001) 5950.
[18] U. Heiz, F. Vanolli, L. Trento, W.-D. Schneider, Rev. Sci. Instrum. 68 (1997) 1986.
[19] T. Engel, G. Ertl, J. Chem. Phys. 69 (1978) 1267.
[20] T. Engel, G. Ertl, Adv. Catal. 28 (1979) 1.
[21] M. Boudard, Adv. Catal. 20 (1969) 153.
[22] I. Stara, V. Nehasil, V. Matolin, Surf. Sci. 331–333 (1995) 173.
[23] J. Libuda, I. Meusel, J. Hoffmann, J. Hartmann, L. Piccolo, C.R. Henry, H.-J. Freund, J. Chem. Phys. 114 (2001) 4669.
[24] L. Piccolo, C. Becker, C.R. Henry, J. E. Phys. D 9 (1999) 415.
[25] C. Becker, C.R. Henry, Catal. Lett. 43 (1997) 55.
[26] C. Becker, C.R. Henry, Surf. Sci. 352 (1996) 457.
[27] M.A. Röttgen, K. Judai, S. Abbet, A. Wörz, C.R. Henry, U. Heiz, in preparation.
[28] K. Okuno, J. Phys. Soc. 55 (1986) 1504.
[29] K. Judai, K. Sera, S. Amatsutsumi, K. Yagi, T. Yasuike, S. Yabushita, A. Nakajima, K. Kaya, Chem. Phys. Lett. 334 (2001) 277.
[30] D.W. Goodman, D.R. Rainer, M. Koranne, S.M. Vesecky, J. Phys. Chem. B 101 (1997) 10769.
[31] Y.T. Malulevich, T.J. Vink, P.A. Zeijlmans van Emmichoven, Phys. Rev. Lett. 89 (2002) 167601.
[32] M.C. Wu, J.S. Corneille, C.A. Estrada, J.-W. He, D.W. Goodman, Chem. Phys. Lett. 182 (1991) 472.
[33] D. Proch, T. Trickl, Rev. Sci. Instrum. 60 (1989) 713.
[34] A.K. Santra, D.W. Goodman, Electrochim. Acta 47 (2002) 3595.
[35] Y. Shi, K.M. Ervin, J. Chem. Phys. 108 (1998) 1757.